



Nonlinear Dynamics of Filaments. III. Instabilities of Helical Rods

A. Goriely; M. Tabor

Proceedings: Mathematical, Physical and Engineering Sciences, Vol. 453, No. 1967
(Dec. 8, 1997), 2583-2601.

Stable URL:

<http://links.jstor.org/sici?sici=1364-5021%2819971208%29453%3A1967%3C2583%3ANDOFII%3E2.0.CO%3B2-L>

Proceedings: Mathematical, Physical and Engineering Sciences is currently published by The Royal Society.

Your use of the JSTOR archive indicates your acceptance of JSTOR's Terms and Conditions of Use, available at <http://www.jstor.org/about/terms.html>. JSTOR's Terms and Conditions of Use provides, in part, that unless you have obtained prior permission, you may not download an entire issue of a journal or multiple copies of articles, and you may use content in the JSTOR archive only for your personal, non-commercial use.

Please contact the publisher regarding any further use of this work. Publisher contact information may be obtained at <http://www.jstor.org/journals/rsl.html>.

Each copy of any part of a JSTOR transmission must contain the same copyright notice that appears on the screen or printed page of such transmission.

JSTOR is an independent not-for-profit organization dedicated to creating and preserving a digital archive of scholarly journals. For more information regarding JSTOR, please contact support@jstor.org.

Nonlinear dynamics of filaments. III

Instabilities of helical rods

BY A. GORIELY^{1,2} AND M. TABOR¹

¹*University of Arizona, Program in Applied Mathematics,
Building #89, Tucson, AZ 85721, USA*

²*Université Libre de Bruxelles, Département de Mathématique,
CP218/1, 1050 Brussels, Belgium*

The time-dependent Kirchhoff equations for thin elastic rods are used to study the linear stability of twisted helical rods with intrinsic curvature and twist. Using a newly developed perturbation scheme, we derive the general dispersion relations governing the stability of various helical configurations. We show that helices with no terminal forces are always dynamically stable. We also compute the most stable helical shape against twist perturbations and show that different unstable modes can be excited in different regions of the parameter space and can sometimes coexist. The linearly unstable modes are computed and explicit forms are given.

1. Introduction

Helices are one of the most simple elementary structures found in nature. They appear at many different level of organization: ranging from molecular biology to magnetohydrodynamics (Barkley & Zimm 1979; Mendelson 1985; Hunt & Hearst 1991; Ricca 1994). The usual approach to modelling these structures is to assume that they can be represented as an elastic filament subject to the classical laws of mechanics and elasticity theory. Within the framework of linear elasticity, the Kirchhoff equations for elastic filaments provide a basic starting point for much analysis and computation (Antman 1995). These equations are a system of coupled nonlinear partial differential equations embodying the conservation of linear and angular momentum in terms of the time and space evolution of a local triad (the director basis) attached to the filament. They have been demonstrated to capture many fundamental features of real elastica and have recently been obtained as the convergent limit of three-dimensional elasticity theory (Ge *et al.* 1996). Stationary (i.e. time independent) helices are known to be exact solutions of the Kirchhoff equations (Love 1892; Timoshenko & Gere 1961; Ziegler 1968) and as a consequence they have been extensively studied, both numerically and theoretically. However, to the best of our knowledge, the *dynamical stability*, that is the growth of time-dependent instabilities, of helical forms has never been investigated. To do so, one has to consider evolution governed by the full time-dependent Kirchhoff equations and this required us to develop a novel arc-length-preserving perturbation scheme (Goriely & Tabor 1997*a, b*). We show here how to apply this general perturbation procedure to the particular case of the helical filaments.

The paper is organized as follows. In §2, we give the basic elements of curve

dynamics and the Kirchhoff model in the general director basis. In §3, we describe the perturbation procedure. In §4, we describe the stationary solutions for helices. In §5, we derive the dynamical variational equations and their associated dispersion relations. Section 6 is devoted to the analysis of these dispersion relations and the construction of the linear solutions after bifurcation.

2. The Kirchhoff model

(a) Kinematics of curves

The Kirchhoff model describes the evolution of elastic filaments. The physically relevant quantities characterizing the three-dimensional elastic body are described in terms of a local coordinate basis attached to the space curve defining the central axis of the filament. We first give a brief summary of the kinematics (i.e. the relationship between positions and velocities) of space curves before describing the dynamics (i.e. the relationship between velocities and forces).

The space curve $\mathbf{x} = \mathbf{x}(s, t) : \mathbb{R} \times \mathbb{R} \rightarrow \mathbb{R}^3$ is parametrized by arc length, s , and time, t , and assumed to be of at least class C^3 . A local coordinate triad $\{\mathbf{d}_1, \mathbf{d}_2, \mathbf{d}_3\}$ is defined for each value of s and t with the vector $\mathbf{d}_3(s, t) = \mathbf{x}'(s, t)$ corresponding to the tangent vector of \mathbf{x} at s . (The prime denotes the s derivative and since s is the arc length it follows that $\mathbf{d}_3 \cdot \mathbf{d}_3 = 1$.) The vectors $\{\mathbf{d}_1(s, t), \mathbf{d}_2(s, t)\}$ are an orthonormal pair defining the plane normal to \mathbf{d}_3 . The three vectors are chosen such that $\{\mathbf{d}_1, \mathbf{d}_2, \mathbf{d}_3\}$ form a *right-handed orthonormal triad* ($\mathbf{d}_1 \times \mathbf{d}_2 = \mathbf{d}_3$, $\mathbf{d}_2 \times \mathbf{d}_3 = \mathbf{d}_1$). If \mathbf{d}_1 is set along \mathbf{d}_3' , the triad specializes to the well-known Frenet frame in which \mathbf{d}_1 and \mathbf{d}_2 are the normal and bi-normal vectors, respectively. The space curve can be reconstructed at all times by integrating the tangent vector, i.e. $\mathbf{x}(s, t) = \int^s \mathbf{d}_3(s, t) ds$.

The considerable advantage of the director basis is that it can be used to represent physical filaments by setting the directors \mathbf{d}_1 and \mathbf{d}_2 to coincide with the principal axes of the rod and, where appropriate, rotate with respect to s along the tangent direction. Their rotation with respect to s along the tangent direction corresponds to the twist in the rod. By contrast, the Frenet basis, which provides a geometrically appealing characterization of space curves, cannot capture satisfactorily such physical properties of actual rods. The evolution of the director basis with respect to arc length and time takes the form

$$\mathbf{d}_i' = \sum_{j=1}^3 K_{ij} \mathbf{d}_j, \quad i = 1, 2, 3, \quad (2.1a)$$

$$\dot{\mathbf{d}}_i = \sum_{j=1}^3 W_{ij} \mathbf{d}_j, \quad i = 1, 2, 3, \quad (2.1b)$$

where $(\dot{\quad})$ stands for the time derivative. W and K are the antisymmetric 3×3 matrices

$$K = \begin{pmatrix} 0 & \kappa_3 & -\kappa_2 \\ -\kappa_3 & 0 & \kappa_1 \\ \kappa_2 & -\kappa_1 & 0 \end{pmatrix}, \quad W = \begin{pmatrix} 0 & \omega_3 & -\omega_2 \\ -\omega_3 & 0 & \omega_1 \\ \omega_2 & -\omega_1 & 0 \end{pmatrix}, \quad (2.2)$$

which ensures that the basis remains orthonormal (Goriely & Tabor 1997a). The

elements of K and W make up the components of the *twist* and *spin vectors*, respectively; namely, $\boldsymbol{\kappa} = \sum_{i=1}^3 \kappa_i \mathbf{d}_i$ and $\boldsymbol{\omega} = \sum_{i=1}^3 \omega_i \mathbf{d}_i$.

(b) *Dynamics of filaments*

The above relations for the evolution of the director basis are pure kinematics and physical dynamics must now be formulated to give the relationship between the strains, κ_i , and the stresses associated with the linear and angular momenta. Kirchhoff's theory of elastic filaments (Dill 1992) is based on the idea that for sufficiently thin rods with modest local deformations, it is possible to describe the forces and moments averaged over local cross-sections attached to the central axis, $\mathbf{x} = \mathbf{x}(s, t)$, of the rod. This enables one to write down a one-dimensional (i.e. parametrized by s) theory. In this framework, the total force $\mathbf{F} = \mathbf{F}(s, t)$ and the total moment $\mathbf{M} = \mathbf{M}(s, t)$ can thus be expressed locally in term of the director basis, i.e. $\mathbf{F} = \sum_{i=1}^3 f_i \mathbf{d}_i$, $\mathbf{M} = \sum_{i=1}^3 M_i \mathbf{d}_i$. Conservation of linear and angular momentum then leads to equations for the force and the moment (Coleman *et al.* 1993)

$$\mathbf{F}' = \rho A \ddot{\mathbf{d}}_3, \tag{2.3 a}$$

$$\mathbf{M}' + \mathbf{d}_3 \times \mathbf{F} = \rho I (\mathbf{d}_1 \times \ddot{\mathbf{d}}_1 + \mathbf{d}_2 \times \ddot{\mathbf{d}}_2), \tag{2.3 b}$$

where I is the moment of inertia (about a radial cross-section), ρ is the density and A the area of a (circular) cross-section. These equations are completed by introducing constitutive relationships. In the *linear* theory of elasticity these take the form

$$\mathbf{M} = EI((\kappa_1 - \kappa_1^u) \mathbf{d}_1 + (\kappa_2 - \kappa_2^u) \mathbf{d}_2) + 2\mu I(\kappa_3 - \kappa_3^u) \mathbf{d}_3, \tag{2.4}$$

where E is Young's modulus, μ the shear modulus and the vector $\boldsymbol{\kappa}^u$ corresponds to the twist (if any) in the unstressed configuration and will be referred to as the *intrinsic twist vector*†. For instance, if $\boldsymbol{\kappa}^u = 0$, the filament is said to be naturally straight, i.e. the lowest energy configuration of the filament is a straight rod. If $\boldsymbol{\kappa}^u = (0, 1/R^u, 0)$, the rod is naturally circular and the lowest energy configuration is a ring of radius R^u . Here, we are defining the (static) energy to be

$$\mathcal{E} = \int \mathbf{M} \cdot (\boldsymbol{\kappa} - \boldsymbol{\kappa}^u) ds. \tag{2.5}$$

Without loss of generality, we can rescale all the variables

$$\left. \begin{aligned} t &\rightarrow t\sqrt{I\rho/AE}, & s &\rightarrow s\sqrt{I/A}, & \mathbf{F} &\rightarrow AEF, & \mathbf{M} &\rightarrow ME\sqrt{AI}, \\ \boldsymbol{\kappa} &\rightarrow \boldsymbol{\kappa}\sqrt{A/I}, & \boldsymbol{\omega} &\rightarrow \boldsymbol{\omega}\sqrt{AE/I\rho}. \end{aligned} \right\} \tag{2.6}$$

and the Kirchhoff equations (2.3)–(2.4) take the form

$$\mathbf{F}' = \ddot{\mathbf{d}}_3, \tag{2.7 a}$$

$$\mathbf{M}' + \mathbf{d}_3 \times \mathbf{F} = \mathbf{d}_1 \times \ddot{\mathbf{d}}_1 + \mathbf{d}_2 \times \ddot{\mathbf{d}}_2, \tag{2.7 b}$$

$$\mathbf{M} = (\kappa_1 - \kappa_1^u) \mathbf{d}_1 + (\kappa_2 - \kappa_2^u) \mathbf{d}_2 + \Gamma(\kappa_3 - \kappa_3^u) \mathbf{d}_3, \tag{2.7 c}$$

where $\Gamma = 2\mu/E$. For rods with circular cross-section, it is a simple matter to show that $\Gamma = 1/(1 + \sigma)$, where σ is Poisson's ratio. The parameter Γ characterizes

† The component $\kappa_3^{(u)}$ is the *intrinsic twist*, whereas $\sqrt{((\kappa_1^{(u)})^2 + \kappa_2^{(u)})^2}$ is the *intrinsic curvature*).

the elastic property of the filament varying between $\frac{2}{3}$ (incompressible case) and 1 (hyper-elastic case). In all the specific examples studied in this paper, $\Gamma = \frac{3}{4}$.

Equation (2.7c) can be used to eliminate \mathbf{M} from (2.7b). The net result, on combining with the twist and spin equations, is a system of nine equations for nine unknowns $(\mathbf{f}, \boldsymbol{\kappa}, \boldsymbol{\omega})$. We refer to this system as the *Kirchhoff equations*. It should be noted that solving (2.7b) only yields the normal components f_1 and f_2 of the force in terms of the strains κ_i and the spins ω_i . The tangential force component f_3 represents the *tension* along the rod and this must be determined by the requirement of arc-length conservation. Overall, the Kirchhoff equations describe the time evolution of a thin rod (here with circular cross-section) in the limit of small deformations where tractions on the external surfaces are assumed to vanish. From now on, the terms *Kirchhoff rod* or simply a *rod* refer to a solution of this set of equations with proper boundary conditions and initial data.

3. Perturbation scheme

Although a considerable amount of analytical work on the Kirchhoff equations is performed in terms of the Euler angles, we have found (Goriely & Tabor 1997a) that the stability of stationary solutions is best described in terms of a perturbation scheme at the level of the local director basis. The idea is to represent the basis of the perturbed system as an expansion around the unperturbed stationary triad such that it remains orthonormal at each order in the perturbation parameter. That is,

$$\mathbf{d}_i = \mathbf{d}_i^{(0)} + \epsilon \mathbf{d}_i^{(1)} + O(\epsilon^2), \quad i = 1, 2, 3. \quad (3.1)$$

Imposition of the orthonormality condition $\mathbf{d}_i \cdot \mathbf{d}_j = \delta_{ij}$ leads to an expression for the perturbed basis in terms of the unperturbed basis; namely,

$$\mathbf{d}_i^{(1)} = \sum_{j=1}^3 A_{ij} \mathbf{d}_j^{(0)}, \quad (3.2)$$

where A is the *antisymmetric* matrix

$$A = \begin{pmatrix} 0 & \alpha_3 & -\alpha_2 \\ -\alpha_3 & 0 & \alpha_1 \\ \alpha_2 & -\alpha_1 & 0 \end{pmatrix}. \quad (3.3)$$

It is straightforward, given the vector $\boldsymbol{\alpha} = (\alpha_1, \alpha_2, \alpha_3)$, to reconstruct the perturbed rod by integrating the tangent vector

$$\mathbf{x}(s, t) = \int^s ds (\mathbf{d}_3^{(0)} + \epsilon(\alpha_2 \mathbf{d}_1^{(0)} - \alpha_1 \mathbf{d}_2^{(0)})) + O(\epsilon^2). \quad (3.4)$$

This type of perturbation expansion can be applied to any vector represented in terms of the \mathbf{d}_i . Thus the vector $\mathbf{V} = \sum_{i=1}^3 v_i \mathbf{d}_i$ can be expanded as $\mathbf{V} = \mathbf{V}^{(0)} + \epsilon \mathbf{V}^{(1)} + O(\epsilon^2)$, where

$$\mathbf{V}^{(1)} = \sum_i (v_i^{(1)} + (A \cdot v^{(0)})_i) \mathbf{d}_i^{(0)}. \quad (3.5)$$

This observation enables us to express the first-order perturbations of the twist and spin matrices, i.e. $K = K^{(0)} + \epsilon K^{(1)} + \dots$, $W = W^{(0)} + \epsilon W^{(1)} + \dots$, where, by using

the kinematic equations (2.1), one may show that

$$K^{(1)} = \frac{\partial A}{\partial s} + [A, K^{(0)}], \tag{3.6 a}$$

$$W^{(1)} = \frac{\partial A}{\partial t} + [A, W^{(0)}] \tag{3.6 b}$$

and $[A, B] = A \cdot B - B \cdot A$. Higher-order perturbations can easily be obtained in terms of the lower-order terms in the same way (Goriely & Tabor 1997b).

The use of this perturbation expansion and the above equations enables one to derive the *dynamical variational equations* by expanding the Newton's equation (2.7 a) and moment equation (2.7 b) to first order in ϵ . These equations are a linear system of six equations for the six-dimensional vector $\boldsymbol{\mu} = \{\boldsymbol{\alpha}, \mathbf{f}^{(1)}\}$,

$$L_E(\boldsymbol{\kappa}^{(0)}, \mathbf{f}^{(0)}) \cdot \boldsymbol{\mu} = 0, \tag{3.7}$$

where $\mathbf{f}^{(1)}$ is the first-order correction to the force and L_E is a second-order differential operator in s and t whose coefficients depend on s through the unperturbed solution $\boldsymbol{\kappa}^{(0)}, \mathbf{f}^{(0)}$. The explicit form of L_E was given in full generality in Goriely & Tabor (1997a). The solutions of the variational equations control the stability, or lack thereof, of the stationary solutions with respect to linear time-dependent modes.

4. The stationary helix

The geometry and statics of helical rods are well known. A more recent study of the energetics of helices is given in Ricca (1995). Here we summarize the results relevant to our stability analysis. We consider a helical space curve, \mathbf{x}_h , wrapped around a cylinder of radius R whose central axis points along the fixed vector \mathbf{e}_1 (i.e. the x -axis)

$$\mathbf{x}_h = (P\delta s, R \cos(\delta s), R \sin(\delta s)). \tag{4.1}$$

Here s is the arc length and δ is determined by the arc length defining constraint $\mathbf{T}(s) \cdot \mathbf{T}(s) = 1, \forall s$, where $\mathbf{T}(s)$ is the tangent vector $\mathbf{T}(s) = \mathbf{x}'_h(s)$. This yields

$$\delta = \pm \sqrt{\frac{1}{P^2 + R^2}}. \tag{4.2}$$

The choice $+$ defines a right-handed helix for $P > 0$. That is, if you point your right-hand thumb along the x -axis, your hand will naturally rotate to the right as you move along the helix. This helix is shown in figure 1. A few additional facts about the helix geometry can be noted at this point. The height (along the x -axis) per turn of the helix is $h = 2\pi P$ and the length of the curve per turn is $l = 2\pi/\delta$. Thus, for a helix of N turns, the total height is $H = 2\pi PN$ and the total filament length is $L = 2\pi N/\delta$.

We can now build the Frenet triad associated with the helix. The normal vector $\mathbf{N}(s)$ is obtained by further differentiating and normalizing the tangent vector, and the binormal vector $\mathbf{B}(s)$ is simply constructed by taking the cross product $\mathbf{B}(s) = \mathbf{N}(s) \times \mathbf{T}(s)$,

$$\mathbf{T}(s) = (P\delta, -R\delta \sin(\delta s), R\delta \cos(\delta s)), \tag{4.3 a}$$

$$\mathbf{N}(s) = (0, -\cos(\delta s), -\sin(\delta s)), \tag{4.3 b}$$

$$\mathbf{B}(s) = (-R\delta, -P\delta \sin(\delta s), P\delta \cos(\delta s)). \tag{4.3 c}$$

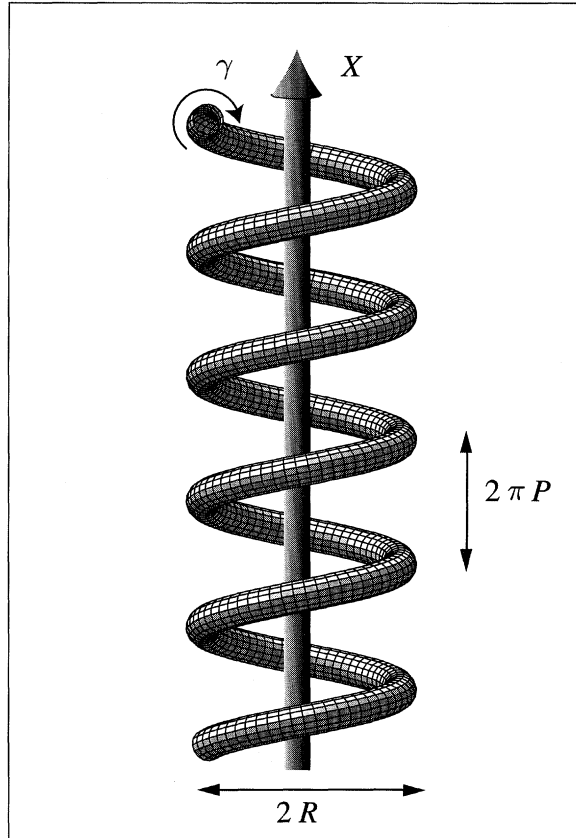


Figure 1. A helical rod characterized by an applied twist γ , a radius R and a loop-to-loop distance $2\pi P$.

The Frenet curvature, κ_F , and torsion, τ_F , are easily shown to be

$$\kappa_F = R\delta^2 = \frac{R}{P^2 + R^2} \tag{4.4 a}$$

$$\tau_F = P\delta^2 = \frac{P}{P^2 + R^2}. \tag{4.4 b}$$

Along with the planar circle and the straight line, the helix is the only geometry for which κ_F and τ_F are constant functions of arc length.

As mentioned earlier, the Frenet triad is merely a special director basis. A more general triad can be constructed by taking $\mathbf{d}_3(s) = \mathbf{T}(s)$ and applying a rotation of angle γ in the normal plane

$$\mathbf{d}_1^{(0)} = \cos(\gamma s)\mathbf{N} - \sin(\gamma s)\mathbf{B}, \tag{4.5 a}$$

$$\mathbf{d}_2^{(0)} = -\sin(\gamma s)\mathbf{N} - \cos(\gamma s)\mathbf{B}, \tag{4.5 b}$$

$$\mathbf{d}_3^{(0)} = \mathbf{T}. \tag{4.5 c}$$

It is now possible to compute the twist vector by substituting this triad in the twist equation (2.1 a) and solving for the unknowns $\boldsymbol{\kappa}^{(0)}$. Doing so, we obtain

$$\boldsymbol{\kappa}^{(0)} = (\kappa_F \sin(\gamma s), \kappa_F \cos(\gamma s), \tau_F + \gamma). \tag{4.6}$$

At this level of description, the angle γ is arbitrary. However, it can be used to ascribe real physical properties to a helical rod (as opposed to curve) by representing the twist (if any) of the rod about its central axis. We will sometimes refer to γ as the *twist density* of the rod. A useful interpretation of (4.6) is to think of the filament as a helical space curve to which is attached a ribbon rotating about the curve with twist density γ . This is the point of view we will adopt here in characterizing helical filaments.

The physical properties of a static helical rod can be determined by solving the time-independent form of the Kirchhoff equations. In this case, since the helix is stationary, we have, trivially, $\omega^{(0)} = 0$ for the spin vector. In the constitutive relations (2.4), it is possible to choose a variety of κ^u . Here we choose the ‘undistorted’ twist vector to correspond to another helix, i.e.

$$\kappa^u = (\kappa_F^u \sin(\gamma^u s), \kappa_F^u \cos(\gamma^u s), \tau_F^u + \gamma^u), \tag{4.7}$$

where κ_F^u and τ_F^u are the Frenet curvature and torsion associated with a helical curve of radius R^u and pitch parameter P^u , and γ^u is a specified twist density. However, in the case of the latter, it is easily demonstrated for the helix that static solutions only exist when the stressed and unstressed twist densities (γ and γ^u , respectively) are the same. This is a consequence of the constancy of the Frenet curvature and torsion.

Knowing the twist vector $\kappa^{(0)}$, we can substitute it into the moment equation (2.7b) and find conditions on the forces $(f_1^{(0)}, f_2^{(0)})$ for a stationary solution and then determine the tension $f_3^{(0)}$ from equation (2.7a). One finds

$$\mathbf{f}^{(0)} = (f_0 \sin(\gamma s), f_0 \cos(\gamma s), (\tau_F/\kappa_F) f_0), \tag{4.8}$$

where

$$f_0 = -\tau_F(\kappa_F - \kappa_F^u) + \Gamma \kappa_F(\tau_F - \tau_F^u) \tag{4.9}$$

and we are assuming that $\kappa_F \neq 0$.

These results exhibit the correct limit for the planar ring, i.e. $P \rightarrow 0$. In the case of the unstressed configuration corresponding to a straight rod, (i.e. $\kappa_F^u = 0$), we write the unstressed curvature vector as $\kappa^u = (0, 0, \gamma^u)$ and note that stationary helical solutions are now possible for $\gamma \neq \gamma^u$. In this case, the forces are found to be $f^{(0)} = (f_0 \sin(\gamma s), f_0 \cos(\gamma s), 0)$, where $f_0 = \tau_F \kappa_F (\Gamma - 1) + \Gamma \kappa_F (\gamma - \gamma^u)$.

In general, it is necessary to apply a terminal force, i.e. an axial force at the ends, to hold the helix in its given shape. However, for special choices of parameters, it is possible to find a ‘free-standing’ helix, namely one for which no such forces are required. It is easily shown that the axial force, i.e. the force f_x along the x -axis, is given by $f_x = f_0 \sec(\alpha)$, where α is the pitch angle defined as $\tan(\alpha) = R/P$. Thus, since the free-standing condition is simply $f_0 = 0$, such a helix can be formed when

$$\kappa_F(\gamma\Gamma - \tau_F(1 - \Gamma)) + \kappa_F^u(\tau_F - \Gamma\kappa_F) = 0. \tag{4.10}$$

For example, if the unstressed configuration is a naturally straight rod (i.e. $\kappa_F^u = 0$), the free-standing condition is $\gamma = \tau_F(1 - \Gamma)/\Gamma$. We note also that even if terminal forces do not need to be applied to the helix, a terminal moment has to be applied to maintain the helical structure. In the case of the naturally straight rod, this is simply $\mathbf{M} = (\kappa_F \sin(\gamma s), \kappa_F \cos(\gamma s), \tau_F(1 - \Gamma))$.

The only way to build a helix requiring no terminal force and no terminal moment is to specify a non-vanishing intrinsic curvature and intrinsic torsion. In this case, $\kappa^u = \kappa^{(0)}$ and the helix has vanishing elastic energy. This case will be referred to as a *naturally free helix*.

5. The dynamical variational equation and the dispersion relation

We now have all the ingredients for a linear analysis of the stationary helix. Substitution of $(\boldsymbol{\kappa}^{(0)}, \mathbf{f}^{(0)})$ into (3.7) gives a six-dimensional system of equations for the six-dimensional vector $\boldsymbol{\mu}$. This system has s -dependent coefficients. In order to obtain a linear system with constant coefficients, we define the new variables $\boldsymbol{\nu} = R_\gamma \cdot \boldsymbol{\mu}$, where

$$R_\gamma = \begin{pmatrix} M_\gamma & 0 \\ 0 & -M_\gamma \end{pmatrix} \tag{5.1}$$

and

$$M_\gamma = \begin{pmatrix} -\cos(\gamma s) & \sin(\gamma s) & 0 \\ \sin(\gamma s) & \cos(\gamma s) & 0 \\ 0 & 0 & -1 \end{pmatrix}. \tag{5.2}$$

The new system is a six-dimensional system with constant coefficients that can be written in the following shorthand form:

$$L_1 \cdot \frac{\partial^2 \boldsymbol{\nu}}{\partial t^2} + L_2 \cdot \frac{\partial \boldsymbol{\nu}}{\partial s} + L_3 \cdot \frac{\partial^2 \boldsymbol{\nu}}{\partial s^2} + L_4 \cdot \boldsymbol{\nu} = 0, \tag{5.3}$$

where L_i are 6×6 matrices whose entries depends upon the parameters $(R, P, \gamma, \Gamma, R^u, \tau)$.

The different linear solutions of this system control the stability and/or vibration modes of the helix. The general solutions of this linear system can be written as a sum of the fundamental linear modes

$$\boldsymbol{\nu}_n = \boldsymbol{\xi}_n e^{\sigma_n t + i \delta n s / N}, \tag{5.4}$$

where $\boldsymbol{\xi}_n \in \mathbb{C}^6$ and N is the total number of turns in the helix ($N \in \mathbb{N}$); that is, we only consider helices with an integral number of loops.

The growth rate σ_n for the n th mode is obtained by requiring that $\boldsymbol{\nu}_n$ is a solution of (5.3),

$$(\sigma_n^2 L_1 + i \delta n L_2 - \delta^2 n^2 L_3 + L_4) \cdot \boldsymbol{\xi}_n \equiv L \cdot \boldsymbol{\xi}_n = 0. \tag{5.5}$$

After some straightforward (but tedious) computation and simplification, the matrix L is found to be

$$\begin{aligned} L_{1,1} &= -2I f_0 \delta^3 \eta / \kappa_F, & L_{1,2} &= -\tau_F (\eta^2 + 1) f_0 \delta^2 / \kappa_F - \sigma^2, & L_{1,3} &= -\delta^2 (\eta^2 + 1) f_0, \\ L_{1,4} &= -\delta^2 (\eta^2 + 1), & L_{1,5} &= 2I \eta \delta \tau_F, & L_{1,6} &= 2I \eta \delta \kappa_F, \\ L_{2,1} &= \tau_F (\eta^2 + 1) f_0 \delta^2 / \kappa_F + \sigma^2, & L_{2,2} &= -2I \tau_F^2 \eta \delta f_0 / \kappa_F, & L_{2,3} &= -2I \tau_F \eta \delta f_0, \\ L_{2,4} &= -2I \tau_F \eta \delta, & L_{2,5} &= -\eta^2 \delta^2 - \tau_F^2, & L_{2,6} &= -\kappa_F \tau_F, \\ L_{3,1} &= \delta^2 (\eta^2 + 1) f_0, & L_{3,2} &= -2I \tau_F \eta \delta f_0, & L_{3,3} &= -2I \kappa_F \eta \delta f_0, \\ L_{3,4} &= -2I \kappa_F \eta \delta, & L_{3,5} &= -\kappa_F \tau_F, & L_{3,6} &= -\eta^2 \delta^2 - \kappa_F^2, \\ L_{4,1} &= (\delta^2 (\Gamma \tau_F^u + \eta^2 \tau_F) + \kappa_F f_0) / \tau_F - \tau_F^2 (\Gamma - 1) + \sigma^2, \\ L_{4,2} &= -I \eta \delta (\tau_F (2 - \Gamma) + \Gamma \tau_F^u), & L_{4,3} &= -I \eta \delta (f_0 + \kappa_F (\tau_F^u \Gamma + \tau_F)) / \tau_F, \\ L_{4,4} &= 0, & L_{4,5} &= 1, & L_{4,6} &= 0, \\ L_{5,1} &= I \eta \delta ((2 - \Gamma) \tau_F + \gamma \tau_F^u), & L_{5,2} &= (1 - \Gamma) \tau_F^2 + \tau_F \tau_F^u \Gamma + \eta^2 \delta + \sigma^2, \end{aligned}$$

$$\begin{aligned}
 L_{5,3} &= ((1 - \Gamma)\tau_F + \Gamma\tau_F^u)\kappa_F, & L_{5,4} &= -1, & L_{5,5} &= 0, & L_{5,6} &= 0, \\
 L_{6,1} &= I\eta\delta(\kappa_F + (f_0 + \tau_F^u\kappa_F\Gamma)/\tau_F)\delta, & L_{6,2} &= \kappa_F^u\tau_F, \\
 L_{6,3} &= (1 - \Gamma)\kappa_F^2 - \tau_F^u\Gamma\tau_F + \Gamma\eta^2\delta^2 + 2\sigma^2 + (\kappa_F f_0 + \Gamma\tau_F^u\delta^2)/\tau_F, \\
 L_{6,4} &= 0, & L_{6,5} &= 0, & L_{6,6} &= 0,
 \end{aligned}$$

where $\eta = n/N$.

The dispersion relation $\Delta = \Delta(\sigma_n, n) \equiv \det(L) = 0$ is a polynomial of degree six in σ_n and of degree 12 in n . Once σ is known for a given n , one can build the corresponding perturbed solutions by finding the null vector ξ_n . The equations (3.4) can then be used to find the perturbed shape. These solutions are always given up to an arbitrary phase corresponding to a rotation of the solution around the x -axis. Setting this phase to zero, we find the deformed mode to first order in ϵ ,

$$\begin{aligned}
 x_1(s, t) &= P\delta s - \frac{2NKR\xi_1}{n\tau_F} \cos\left(\frac{n\delta s}{N}\right), \\
 x_2(s, t) &= R \cos(\delta s) - \frac{K}{\delta} \left[\frac{\xi_2 - \xi_1}{n - N} \sin\left(\frac{n - N}{N}\delta s\right) + \frac{\xi_2 + \xi_1}{n + N} \sin\left(\frac{n + N}{N}\delta s\right) \right], \\
 x_3(s, t) &= R \sin(\delta s) - \frac{K}{\delta} \left[\frac{\xi_2 - \xi_1}{n - N} \cos\left(\frac{n - N}{N}\delta s\right) - \frac{\xi_2 + \xi_1}{n + N} \cos\left(\frac{n + N}{N}\delta s\right) \right],
 \end{aligned}$$

where $K = \epsilon C e^{\sigma t}$ and

$$\begin{aligned}
 \xi_1 &= n^3\tau_F\delta^3\{(n^2 - N^2)^2\delta^6[\kappa_F^2n^2\Gamma + \kappa_F\kappa_F^u(n^2 - 2N^2 + 2\Gamma N^2) + N^2(\kappa_F^u)^2] \\
 &\quad + (n^2 - N^2)^2N^2\kappa_F\delta^4[2\kappa_F^2(\kappa_F^u - \Gamma) + \kappa_F(\sigma^2\Gamma - (\kappa_F^u)^2) + \kappa_F^u(\sigma^2 - \tau_F\tau_F^u\Gamma)] \\
 &\quad + N^4\sigma^2\kappa_F\delta^2[\kappa_F\Gamma(N^2 + n^2) + \kappa_F^u(3N^2 + n^2)] - 2\sigma^2N^6\kappa_F^u\kappa_F\}, \\
 \xi_2 &= -Nn^4\delta^2\{\delta^6[\kappa_F^2\Gamma(n^2 - N^2)(\tau_F(2 - \Gamma) + \tau_F^u) + \kappa_F\kappa_F^u(n^2 - N^2)(\tau_F(1 - \Gamma) + \tau_F^u\Gamma) \\
 &\quad + (\kappa_F^u)^2\tau_FN^2(2N^2 - n^2)] + N^3n^2\kappa_F\kappa_F^u\tau_F\delta^4[\kappa_F^2(\Gamma - 1)(n^2 - N^2) \\
 &\quad + \sigma^2(n^2 - N^2) + 3\kappa_FN^4\kappa_F^u] + N^5n^2\kappa_F\tau_F\delta^2[-3\kappa_F^3\kappa_F^uN^2 + 2\kappa_Fn^2\sigma^2\Gamma \\
 &\quad + \kappa_F^u\sigma^2(3n^2 - N^2)] + N^7\tau_F\kappa_F^u[\kappa_F^6\kappa_F^u n^2 - \kappa_F^3\sigma^2(3n^2 - N^2) + \kappa_F^u\tau_F^6n^2]\}.
 \end{aligned}$$

6. Linear analysis of the helical filament

We now turn to the stability analysis of the helical filament and consider different settings in which different parameters are varied. We first consider the simplest case where the rod is naturally straight and untwisted and show that the helical conformation is always unstable. To stabilize the rod we include the effects of intrinsic curvature and intrinsic torsion. We will then consider a situation where a stable rod can be destabilized by varying certain control parameters.

We stress at this point that we only consider $\sigma \in \mathbb{R}$. Indeed, the dispersion relation has other solutions corresponding to *vibration modes* (i.e. $i\sigma \in \mathbb{R}$). These modes are not spontaneously unstable. That is, the corresponding amplitude of the linear modes is at most of the size of the perturbations themselves. Therefore, in order to observe these modes, they have to be specifically excited.

The boundary conditions are chosen such that the x_1 component of the helix is fixed in space. In turn, this implies that n is an integer. That is, we only consider here discrete modes of perturbation.

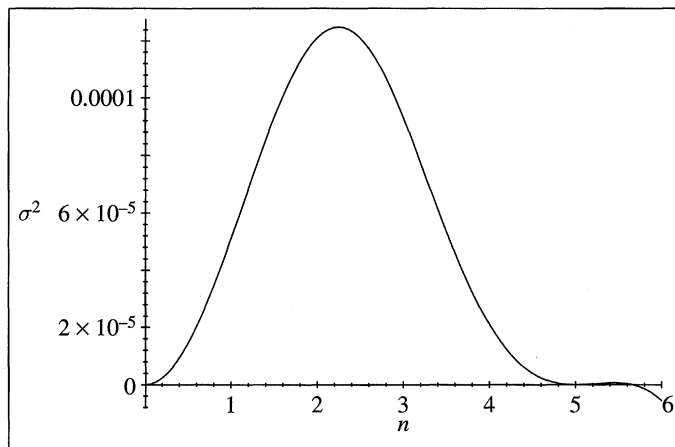


Figure 2. The growth rate σ^2 solution of the dispersion relation for the (naturally straight) helical rod as a function of the spatial mode n . The maximum is obtained close to $n = 2$ ($\kappa_F = \frac{1}{8}$, $\tau_F = \frac{1}{8}$, $N = 5$).

(a) *Instability of a naturally straight helix*

The simplest case we can study is that of an untwisted naturally straight rod shaped as a helix. The intrinsic curvature and the twist density are both set to zero, i.e. $\kappa^u = (0, 0, 0)$ and $\gamma = 0$. In order to show the instability of such a configuration we study the dispersion relation to find the neutral modes and determine if the modes in the range $0 < n/N < 1$ are unstable (that is, $\sigma_n^2 > 0$). The neutral modes are found by setting $\sigma = 0$ in the dispersion relation. The following three neutral modes are found:

$$\left(\frac{n}{N}\right)^2 = 0, \quad \left(\frac{n}{N}\right)^2 = 1, \quad (6.1a)$$

$$\left(\frac{n}{N}\right)^2 = ((\Gamma - 2)^2 \tau_F^2 + \kappa_F^2) \delta^{-2} > 1. \quad (6.1b)$$

Around $n/N = 1$ the exponent σ can be expanded in powers of n ,

$$\sigma^2 = (1 - \Gamma) \delta^4 \left(\frac{n}{N} - 1\right)^2 + O\left(\left(\frac{n}{N} - 1\right)^4\right). \quad (6.2)$$

Since there is no neutral mode between $n/N = 0$ and $n/N = 1$ and locally $\sigma > 0$ around $n = 1$, we conclude that $\sigma_n > 0$ for all modes between $n = 1$ and $n = N - 1$. A typical plot of the dispersion relation is shown in figure 2.

If a naturally straight rod is maintained in a helical shape and suddenly released, toward what shape will it evolve? All the modes from $n = 1$ to $N - 1$ can be destabilized. If the helix has more than one turn ($N > 1$), the helix will be unstable. The mode selected in such an unstable process is the fastest growing mode (it is the one that will be first observed since it grows faster than the others). This mode can be easily found by looking at the integer closest to the maximum of the dispersion relation. For instance, in figure 2, the mode $n = 2$ is close to the maximum. Therefore, the fastest unstable mode is $n = 2$. The integration of the linear equation can be explicitly performed and the solution for the space curve is found by integrating (3.4). Such an unstable mode is shown in figure 3. We see that the instability tends to localize the deformation in two nodes where buckling occurs.

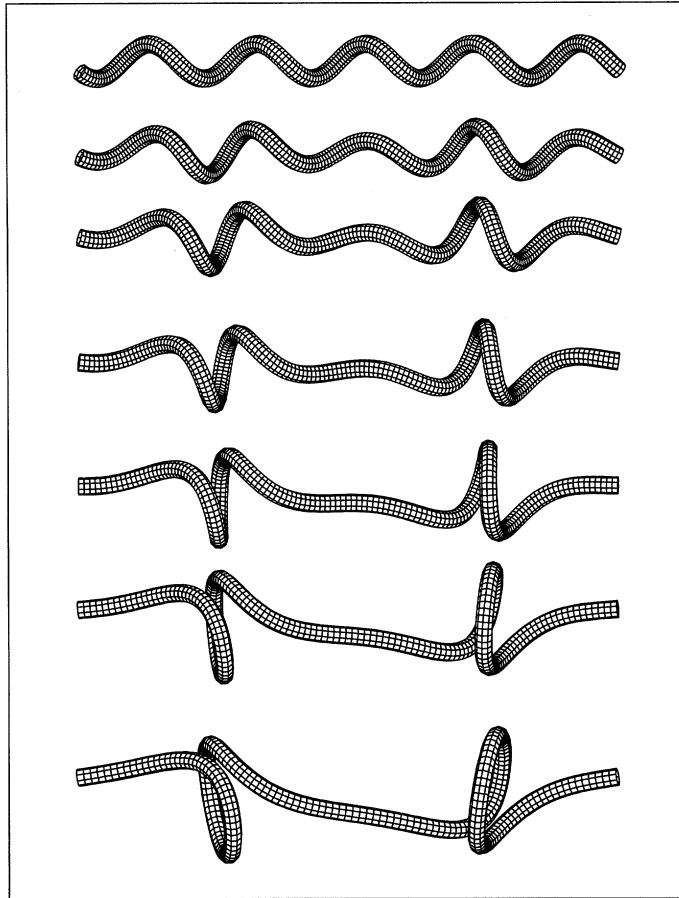


Figure 3. The time evolution of an unstable (naturally straight) helix. The mode $n = 2$ creates two loops ($\kappa_F = \frac{1}{8}$, $\tau_F = \frac{1}{8}$, $N = 5$ and $\frac{1}{1000}K = 0, 2, 4, 6, 8, 10, 12$).

Depending on the control parameters, different modes can become the fastest growing mode. At this point, it should be stressed that the instabilities a helix can undergo are quite different from those found for the planar twisted ring (Zajac 1962; Goriely & Tabor 1997a; Coleman *et al.* 1996) since, in that case, $N = 1$ and the periodic conditions enforced by closure of the ring are such that the only unstable modes are n integer with $n > 1$.

(b) *Stability of intrinsically curved helices*

We now consider helices with intrinsic curvature ($\kappa_F^u \neq 0$) and torsion ($\tau_F^u \neq 0$). Furthermore, we assume that the helix is free-standing; that is, $\kappa = \kappa^u$. The helix is thus in an equilibrium state, since the elastic energy vanishes identically. We expect such a configuration to be also dynamically stable and indeed no unstable mode can be excited. An easy way to show this is to consider the neutral modes. In this simple case, the neutral dispersion relation is

$$\Delta(\sigma = 0) = \Gamma \frac{n^4}{N^4} \delta^{12} \left(1 - \frac{n^2}{N^2} \right)^4. \tag{6.3}$$

The only neutral modes are $n/N = 0$ and $n/N = \pm 1$. At $n/N = \pm 1$, the dispersion

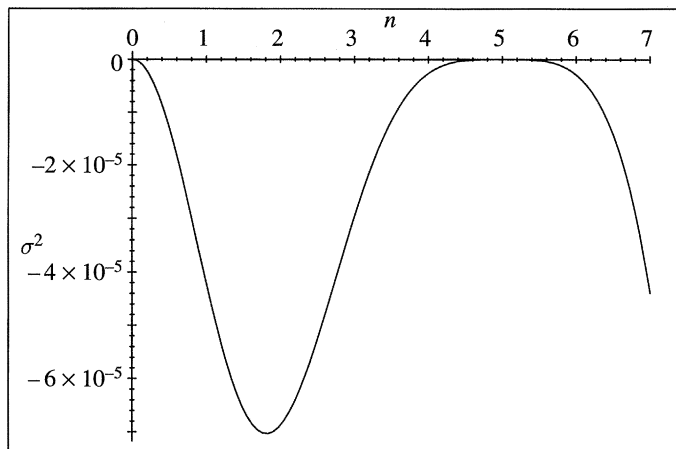


Figure 4. The growth rate σ^2 solution of the dispersion relation for the stable helix as a function of the spatial mode n ($\kappa_F = \frac{1}{8}$, $\tau_F = \frac{1}{8}$, $N = 5$).

relation can be locally expanded,

$$\sigma^2 = -\frac{2\delta^2\tau_F^{-2}}{\Gamma(\delta^2 + \tau_F^2) + \kappa_F^2} \left(\frac{n}{N} - 1\right)^4 + O\left(\left(\frac{n}{N} - 1\right)^8\right). \quad (6.4)$$

Therefore, we conclude that $\sigma^2 \leq 0 \forall n$; that is, no mode is unstable (see figure 4). Nevertheless, as mentioned earlier, the helix can still be subject to vibrations. These vibrations correspond to marginally unstable modes characterized by $\sigma^2 < 0$. Their amplitude is of the same order as the perturbation itself. For each of these unstable modes the frequency can be obtained as $\nu = \sqrt{-\sigma^2}$. These modes probably deserve further investigation.

(c) Stability threshold of free-standing helices

We have seen that *all free helices are stable*. Can we destabilize these structures by varying some of the parameters? There are two different ways a stable helix can be made unstable. First, one can modify ‘external’ parameters such as the curvature or torsion (of the axial curve). For instance, consider the following experiment. Take a free-standing helix and push (or pull and twist) the extremities. The helix will reach a critical shape where it will suddenly become unstable. What is the critical force that one has to exert on the helix to make it unstable and does this force depend on the length of the helix? Towards what shape will it evolve? We will show that the critical shape can easily be computed and that longer helices are indeed easier to destabilize.

The second way a helix can be made unstable is to change the ‘internal’ parameters such as the intrinsic curvature or torsion. While this situation may at first seem rather unphysical (after all, one does not expect the intrinsic characteristics of a rod to vary), there are contexts in which this occurs. For example, in many biological and chemical systems (such as DNA molecules), the external environment (such as pressure and temperature) directly influences the intrinsic characteristics of a filament. By contrast, the external parameters, such as R and P , are much harder to control since it is extremely difficult to actually hold the extremities of a naturally occurring, microscopic, filament and pull it!

It is clear that by varying internal parameters, the helix will eventually become

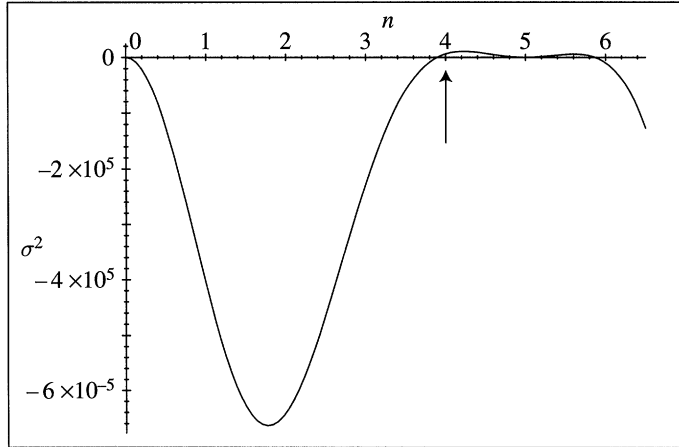


Figure 5. The growth rate σ^2 solution of the dispersion relation for the pushed helix as a function of the spatial mode n . The arrow indicates the first unstable mode ($\kappa^u = \frac{1}{8}$, $\tau^u = \frac{1}{8}$, $R = 4$, $P = \frac{37}{10}$, $N = 5$).

unstable. Indeed, we have seen that setting the intrinsic curvature vector to zero makes the helix unstable. This suggests that there must be a critical intrinsic curvature where the helix first becomes unstable. What is the type of this instability? Should we expect the same kind of behavior as exhibited by a helix which is destabilized as a result of an external adjustment, e.g. pushing? Surprisingly, the instability generated by adjusting internal parameters is, in many respects, different from that seen as a consequence of external changes. For instance, the former will not, in general, depend strongly on the length of the helix. We will now discuss these instabilities in more detail.

(i) *Pushing and pulling helices*

We consider a free-standing helix that is gently pulled (or pushed) until it reaches an unstable point. We assume that the helix has N turns and that the act of pulling or pushing is such that the Frenet curvature and torsion vary away from their equilibrium values. According to equation (4.9), a terminal force f_0 has to be imposed in order to change the shape of the helix. The sign of f_0 determines whether the helix is pushed ($f_0 < 0$) or pulled ($f_0 > 0$). The helix will become unstable if locally the dispersion relation around $n/N = 1$ becomes positive. This can be tested easily by expanding the dispersion relation around this point,

$$\sigma^2 = -f_0 \frac{\delta^4}{\kappa_F \tau_F} \left(\frac{n}{N} - 1 \right)^2 + O\left(\left(\frac{n}{N} - 1 \right)^4 \right). \tag{6.5}$$

From this relation, we conclude that the effect of pulling a helix is to stabilize it, whereas pushing the helix will create locally unstable modes around $n = N$. Let us consider the latter situation. For simplicity, we consider a helix with constant radius and pushed in such a way that only the pitch angle is modified. To do so, we fix $R = R^u$ and modify $P = P^u + P_1$. The parameters (R^u, P^u) corresponds to the stable helix and are related to κ_F and τ_F . The helix will become unstable as soon as $\Delta(\sigma_{N-1} = 0) = 0$. Indeed, the first possible mode to be excited corresponds to the mode $n = N - 1$. A typical dispersion relation is shown in figure 5.

In figure 6, the critical value of the pitch parameter shift P_1 (where $P = 4 + P_1$) is

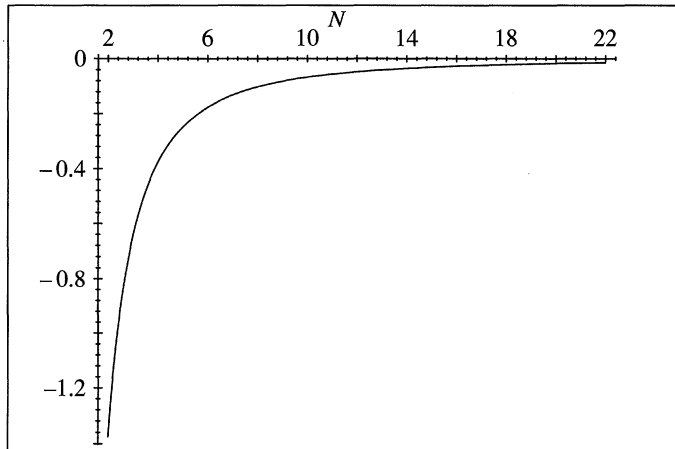


Figure 6. The critical value of P_1 for which the helix becomes unstable as a function of the number of helical turn ($\kappa^u = \frac{1}{8}$, $\tau^u = \frac{1}{8}$, $R = 4$, $P = 4 + P_1$).

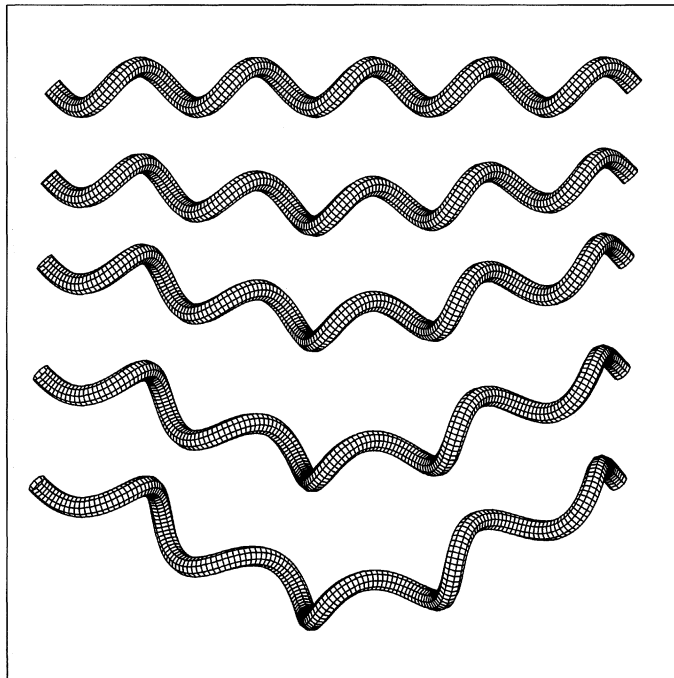


Figure 7. The time evolution of an unstable helix pushed at the extremities ($\kappa^u = \frac{1}{8}$, $\tau^u = \frac{1}{8}$, $R = 4$, $P = \frac{37}{10}$, $N = 5$, $\frac{1}{10}K = 0, 15, 30, 45, 60$).

shown against the number of helical turns N . We see that as the number of helical turns is increased the instability is triggered almost as soon as the helix is pushed. This situation is analogous to the case of a straight elastic rod that becomes unstable as its extremities are pushed. This creates the well-known effect of bending (Love 1892) of beams. The bending of a helix is shown in figure 7.

Pulling a helix stabilizes it. However, a helix under tension can become unstable by increasing its twist. This situation is in many ways analogous to the case of a twisted straight rod under extension: in this case, there exists a critical twist for which the

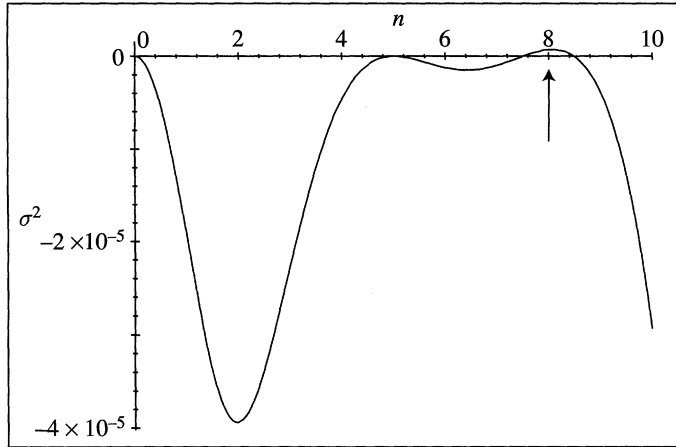


Figure 8. The growth rate σ^2 solution of the dispersion relation for a twisted helix in extension as a function of the spatial mode n ($\kappa^u = \frac{1}{8}$, $\tau^u = \frac{51}{40}$, $R = 4$, $P = 8$, $N = 5$).

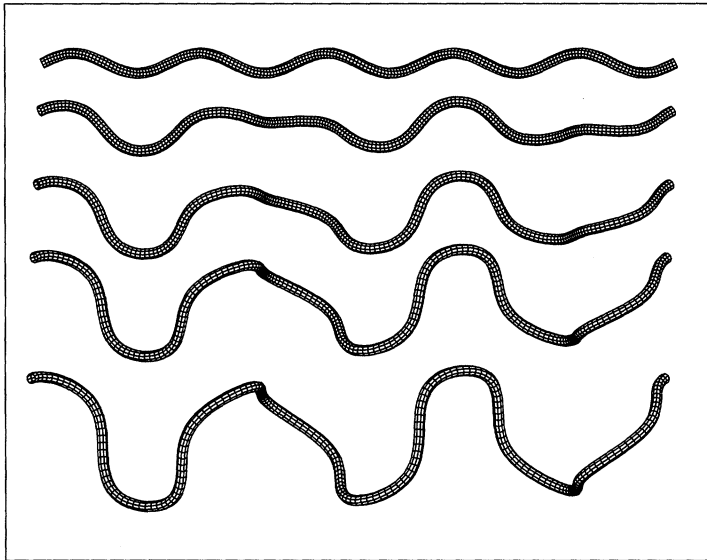


Figure 9. The time evolution of an unstable pulled and twisted helix ($\kappa^u = \frac{1}{8}$, $\tau^u = \frac{51}{40}$, $R = 4$, $P = 8$, $N = 5$, $\frac{1}{100}K = 0, 2, 4, 6, 8$).

twisted rod becomes unstable (Goriely & Tabor 1996, 1997*b*). The values of n and γ for which a (helical) filament becomes unstable can be obtained by solving, for a given force f_0 , the coupled relations

$$\Delta(\sigma_n = 0) = 0 \quad \text{and} \quad \frac{\partial \sigma_n}{\partial n} = 0. \tag{6.6}$$

This leads to a system of two polynomial equations in n and γ that can be solved for a given configuration (a general, explicit, form of the critical mode and twist seems elusive). As an example, the dispersion relation of a twisted, pulled, helix is shown in figure 8, where the mode $n = 8$ is unstable. The corresponding evolution of the helix is shown in figure 9.

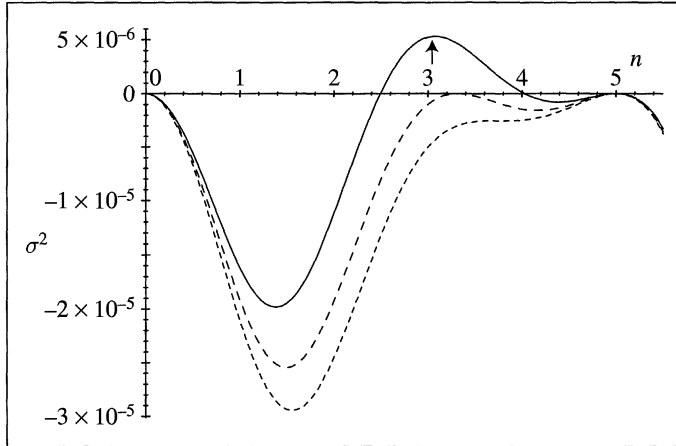


Figure 10. The dispersion relation for a twisted helix in extension. The lower dashed curve ($\kappa_F^u = 0.062$) corresponds to a stable helix. The upper curve ($\kappa_F^u = 0.055$) corresponds to values at which the mode $n = 3$ is unstable. The intermediate curve ($\kappa_F^u = 0.059233$) is the point at which σ^2 is first tangent to the axis ($\tau^u = 0$, $\tau_F = \frac{1}{8}$, $\kappa_F = \frac{1}{8}$, $N = 5$).

(ii) Instabilities of helices with respect to intrinsic curvature

We now turn our attention to the case where the external parameters are fixed and the intrinsic curvature is varied. This situation is in many respects different from the ones just considered. Indeed, the helix has a fixed shape but the intrinsic curvature is varied in such a way that the elastic energy is increased. In a dissipative medium and for small perturbations, the helix would probably return to a new equilibrium shape determined by the elastic energy. However, there is no dissipation at the level of the Kirchhoff equations and the filament is free to evolve. In order to see how the filament is deformed we have to find which mode is first excited. This again amounts to looking at the zeroes of the dispersion relation. To illustrate the kind of behavior that might be expected, we consider the particular case of $\tau_F = \frac{1}{8}$ and $\kappa_F = \frac{1}{8}$. The intrinsic torsion is set to zero ($\tau_F^u = 0$) and we vary κ_F^u from $\frac{1}{8}$ to 0 where the helix is known to be unstable. The different solutions of the dispersion relation for varying values of κ_F^u are shown in figure 10 and the corresponding time evolution of the helix is shown in figure 11. We see that the helical filament deforms into a three loop configuration.

7. Conclusions

The helix is one of the most fundamental spatial configurations and also one of the simplest solutions of the Kirchhoff equations. However, despite much attention in the classical elasticity literature, a stability analysis of the different dynamical perturbations has not, to the best of our knowledge, been achieved. We believe that one of the primary reasons is that much, if not all, of the previous studies have been performed in the setting of stationary perturbations. Using Euler angles, it might be possible to find the value of the parameters for which new solutions may exist. However, even in the case of the planar ring, this is a strenuous task. The development of a perturbation scheme taking into account both time and space dependence allows us to derive the explicit (and completely general) dispersion relation for the helical filament with intrinsic curvature and twist. In the setting of a *dynamical study*, the

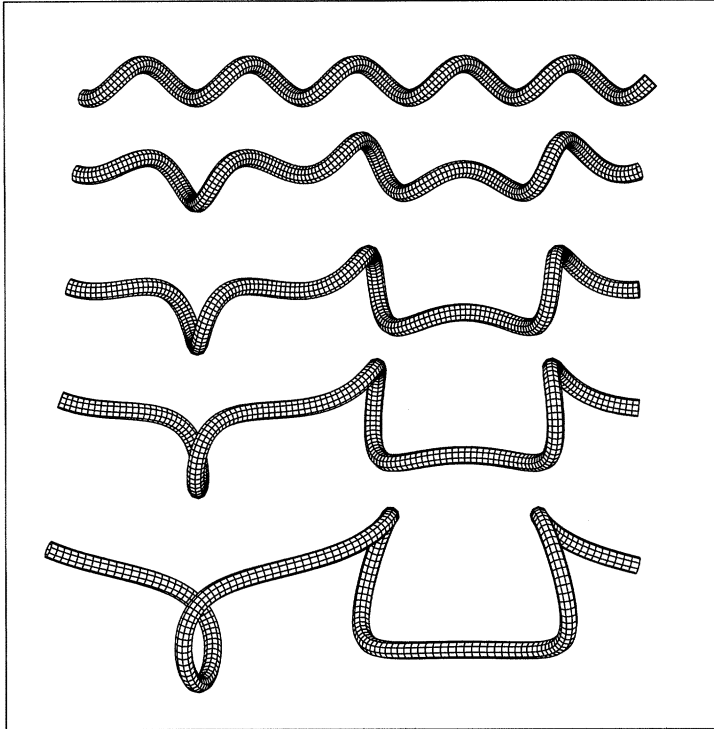


Figure 11. The time evolution of an unstable helix with intrinsic curvature ($\tau^u = 0$, $\kappa^u = 0.055$, $\tau_F = \frac{1}{8}$, $\kappa_F = \frac{1}{8}$, $N = 5$, $n = 3$, $\frac{1}{100}K = 0, 10, 20, 30, 45$).

critical values of the parameters leading to an instability can be readily found as the zeroes of the dispersion relation. This provides a transparent interpretation of the instabilities that a stationary analysis cannot provide without a complementary energy analysis.

Another reason might be purely computational. As seen here, the different relations found in this paper can be extremely cumbersome and it is only thanks to extensive symbolic computation that we were able to analyze the different unstable modes. The advantage of such a powerful tool becomes manifest in this kind of computation.

The linear analysis gives a picture of the way stationary solutions lose their stability. The new solutions give a qualitative picture of the behavior after the bifurcation. However, due to their exponential dependence, these solutions become rapidly unbounded and the linear approximation breaks down. Indeed, as the amplitudes of the linear modes grow, the nonlinear terms can no longer be neglected in the analysis. In order to circumvent this difficulty, a nonlinear analysis needs to be performed. Such an analysis introduces the distance from the bifurcation point as a new small parameter which is then used to introduce new time and arclength scales in the problem on which the arbitrary amplitudes of the linear mode(s) can vary. Within these approximations one can, in the best cases, derive amplitude equations describing the nonlinear interaction between the different amplitudes of the linear modes. Usually, this approach gives a good description of the solution after the bifurcation. In Goriely & Tabor (1997*b*), we show how to perform this analysis in the setting of the Kirchhoff equation for the twisted straight rod. The helical filament can probably be studied in the same way, especially in those cases where the graph of the exponent

σ_n^2 is parabolic around the neutral state (that is, $\sigma_n^2 = -\alpha(n - n_c)^2$ for a certain α). However, the complexity of the higher-order terms in the perturbation expansion presents a formidable computational challenge.

We have identified different regions of parameter space where a helical filament can become unstable. In particular, we explored three different scenarios leading to unstable filaments. In the first case, the helix is pushed. The resulting instability correspond to a bending of the entire helix, much like the bending of a straight rod. The unstable modes are located around the principal neutral mode $n = N$, so that the instability occur at the scale of the helix itself (see figure 7). The second situation arises when the helix is pulled and twisted. In this case, a *higher* mode n_c is excited and the helix deforms throughout the rod by creating $n_c > N$ loops along the helix. These two cases are analogous to the possible deformation of a twisted straight rod and constitute, in some sense, a discrete version of it. A completely different scenario is found by considering the case where the external parameters are held fixed but the intrinsic curvature is changed. Then, the helix undergoes unstable deformations by exciting *lower* modes $n_c < N$. This leads to the intriguing possibility of buckle formation as shown in figure 3. The dynamical formation of buckle in a twisted rod is a commonly observed phenomenon and many experimental works have been dedicated to the problem (Thompson & Champneys 1996). However, to the best of our knowledge, no dynamical description of this looping instability has been proposed. The nonlinear analysis of the unstable rod might well provide such a description (Goriely & Tabor 1997c).

This work is supported by DOE grant DE-FG03-93-ER25174. The authors thank Giacomo Ehrenfreud and Irwin Tobias for emphasizing the importance of applying the dynamical linear analysis to helical filaments.

References

- Antman, S. S. 1995 *Nonlinear problems of elasticity*. Berlin: Springer.
- Barkley, M. D. & Zimm, B. H. 1979 Theory of twisting and bending of chain macromolecules; analysis of the fluorescence depolarization of DNA. *J. Chem. Phys.* **70**, 2991–3006.
- Coleman, B. D., Dill, E. H., Lembo, M., Lu, Z. & Tobias, I. 1993 On the dynamics of rods in the theory of Kirchhoff and Clebsch. *Arch. Ration. Mech. Anal.* **121**, 339–359.
- Coleman, B. D., Lembo & Tobias, I. 1996 A new class of flexure-free torsional vibrations of annular rods. *Mechanica* **31**, 565–575.
- Dill, E. H. 1992 Kirchhoff's theory of rods. *Arch. Hist. Exact. Sci.* **44**, 2–23.
- Ge, Z., Kruse, H. P. & Marsden, J. E. 1996 The limits of Hamiltonian structures in three dimensional elasticity, shells and rods. *J. Nonlinear Sci.* **6**, 19–58.
- Goriely, A. & Tabor, M. 1996 New amplitude equations for thin rods. *Phys. Rev. Lett.* **77**, 3537–3540.
- Goriely, A. & Tabor, M. 1997a Nonlinear dynamics of filaments. I. Dynamical instabilities. *Physica D* **105**, 20–44.
- Goriely, A. & Tabor, M. 1997b Nonlinear dynamics of filaments. II. Nonlinear analysis. *Physica D* **105**, 45–61.
- Goriely, A. & Tabor, M. 1997c Nonlinear dynamics of filaments. IV. Spontaneous looping of twisted rods. *Proc. R. Soc. Lond. A* (Submitted.)
- Hunt, N. G. & Hearst, J. E. 1991 Elastic model of DNA supercoiling in the infinite length limit. *J. Chem. Phys.* **12**, 9329–9336.
- Love, A. E. H. 1892 *A treatise on the mathematical theory of elasticity*. Cambridge University Press.
- Proc. R. Soc. Lond. A* (1997)

- Mendelson, N. H. 1985 A model of bacterial DNA segregation based upon helical geometry. *J. Theor. Biol.* **112**, 25–39.
- Ricca, R. L. 1994 The effect of torsion on the motion of a helical vortex filament. *J. Fluid. Mech.* **273**, 241–259.
- Ricca, R. L. 1995 The energy spectrum of a twisted flexible string under elastic relaxation. *J. Phys. A* **28**, 2335–2352.
- Thompson, J. M. T. & Champneys, A. R. 1996 From helix to localized writhing in the torsional post-buckling of elastic rods. *Proc. R. Soc. Lond. A* **452**, 117–138.
- Timoshenko, S. P. & Gere, J. M. 1961 *Theory of elastic stability*. New York: McGraw-Hill.
- Zajac, E. E. 1962 Stability of two planar loop elasticas. *Trans. ASME*, March, 136–142.
- Ziegler, H. 1968 *Principles of structural stability*. Waltham, MA: Blaisdell.

Received 25 November 1996; accepted 12 May 1997